East European Journal of Physics. 4. 18-30 (2021)
DOI: 10.26565/2312-4334-2021-4-02 ISSN 2312-4334

COMPARISON OF ANATASE AND RUTILE FOR PHOTOCATALYTIC APPLICATION: THE SHORT REVIEW †

Volodymyr Morgunov[*,a,b], **Serhii Lytovchenko**[a], **Volodymyr Chyshkala**[a], **Dmytro Riabchykov**[a], **Dementii Matviienko**[a]

[a] *V. N. Karazin Kharkiv National University, 4 Svobody Sq., Kharkiv, 61022, Ukraine;*

[b] *Ukrainian Engineering Pedagogic Academy, vul. Universitets'ka, 16, Kharkiv, 61003, Ukraine*

**Corresponding Author: v.morgunov@karazin.ua*

Received June 30, 2021; revised August 8, 2021; accepted September 16, 2021

The dioxide titanium (TiO_2) is attracting a great attention as semiconductor photocatalyst because of its high photoreactivity, non-toxicity, corrosion resistance, photostability, cheapness. It can be used in wide range of applications: air and water purification, hydrogen (H_2) generation, CO_2 reduction, in photovoltaic application and others. The efforts of scientists were applied to use solar light for dioxide titanium photocatalysis and to enhance the photocatalytic efficiency. In this article we review the properties difference of anatase and rutile modifications of TiO_2. The anatase has a higher photoefficiency. The higher photoefficiency of anatase is due to longer lifetime of charge carriers (lifetime of e^-/h^+ in anatase on 3 order higher than in rutile). But anatase has higher band gap energy (3.2 eV or 388 nm) in comparison with rutile (3.0 eV or 414 nm). Thus, anatase becomes photosensitive in ultraviolet (UV) diapason of light, meanwhile rutile - in violet spectrum of visible light. It is desirable to obtain TiO_2 semiconductor with properties combining best ones from anatase and rutile: higher photoreactivity and smaller band gap. It can be made by using external factors such as electric or magnetic fields, doping and etc.

Keywords: photocatalysis, dioxide titanium, anatase, rutile, band gap, photoefficiency, electron-hole generation.
PACS: 31.10.+z; 71.20.Nr ; 73.20.-r

INTRODUCTION

The photocatalytic properties of TiO_2 was firstly reported in 1972 [1]. After that an interest of researchers from whole the world to photocatalysis was attracted. On the fig. 1 it can be seen that the number of the publications from the 70s until 2020 has significantly increased. This can be explained by the following reasons:

- a wide range of TiO_2 photocatalyst applications:
  - environmental: purification of water and air, CO_2 reduction [2–7];
  - antibacterial and antimicrobial properties [8–11]
  - energy: electricity and hydrogen production [12–16];
  - self-cleaning material and antifogging [17–20];
- high photoreactivity (usually up to ζ (photonic efficiency) = 10 %)
- chemically and biologically inert and non-toxic;
- inexpensive;
- corrosion resistant and photostable [21, 22].

On the other hand, the disadvantages are the following [3, 15]:

- low photon utilization efficiency and slow removal rate;
- rapid recombination of photo-generated electron/hole pairs;
- the poor activation of TiO_2 by visible light.

†**Cite as:** V. Morgunov, S. Lytovchenko, V. Chyshkala, D. Riabchykov, and D. Matviienko, East. Eur. J. Phys. 4, 18 (2021), https://doi.org/10.26565/2312-4334-2021-4-02.

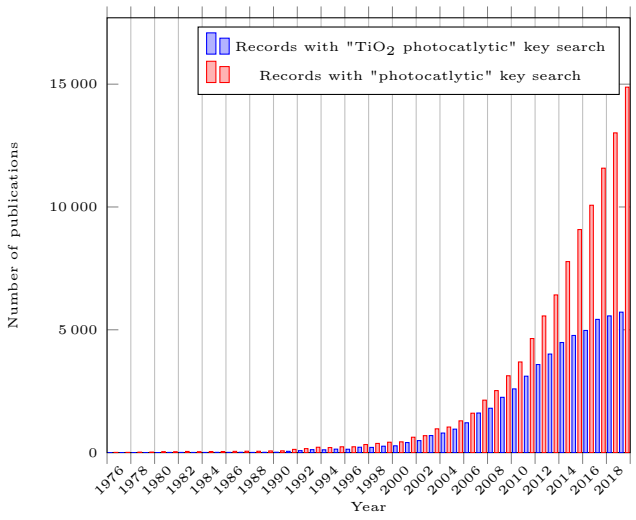

Figure 1: Number of publications of photocatalysis-related and TiO_2 photocatalysis-related papers for the period 1976 - 2020 years. (Source: Web of Science; date: June 9, 2021; keywords: "photocatalytic" and "TiO_2 photocatalytic".)

To solve first issue the nanosized particles of photocatalyst are used.

To reduce recombination electron/hole pairs (second items) some investigators added sacrificial reagents and carbonate salts [15, 23], doped with metals/non-metals [23, 24], loaded noble metal nanoparticles [25, 26] or applied external electrical field [27, 28].

To use visible light for the enhancement photocatalysis (third issue) some investigations focused on modification of TiO_2 by means of metal loading, metal ion doping, dye sensitization, anion doping and metal ion-implantation [29–36].

The aim of this short review is to summarize what was made in this field and elaborate an direction for further investigations.

THEORETICAL ASPECTS OF TIO_2 PHOTOCATALYSIS

We briefly consider the TiO_2 lattice structure and the theory of the photocatalysis. Photocatalysis is complicated phenomena and even definition this phenomena has several version [37]. IUPAC Commissions defined photocatalysis as “a catalytic reaction involving light absorption by a catalyst or a substrate” [38]. In a later revised glossary a complementary definition of a photo-assisted catalysis was also proposed: “catalytic reaction involving production of a catalyst by absorption of light” [39]. And in version of 2011 definition of photocatalysis sounds as following "Change in the rate of a chemical reaction or its initiation under the action of ultraviolet, visible, or infrared radiation in the presence of a substance—the photocatalyst—that absorbs light and is involved in the chemical transformation of the reaction partner" [40]. But more practical definition is "Photocatalysis is phenomena that accelerated chemical reaction in the presence of catalyst which absorbed photons".

A detailed knowledge of the surface structure is the crucial first step in obtaining a detailed knowledge of reaction mechanisms on the molecular scale.

The crystal structure of pure titanium lattice is hexagonal close-packed. The lattice constants of Ti have been determined as [41]

$$a_0 = 2.95111 \pm 0.000\,06\ \text{Å}$$
$$c_0 = 4.68433 \pm 0.000\,10\ \text{Å}$$
$$c/a = 1.5873$$

for a temperature of 25 °C.

Ti hexagonal alpha form changes into a body-centered cubic (lattice) beta form at 882 °C [42].

Titanium dioxide crystallizes in three major different structures:

- rutile (tetragonal, $D_{4h}{}^{14}$-$P4_2/mnm$, a=b=4.584 Å, c=2.953 Å [43]);
- anatase (tetragonal, $D_{4h}{}^{19}$-$I4_1/amd$, a=b=3.782 Å, c=9.502 Å [44]);
- brookite (rhombohedrical, $D_{2h}{}^{15}$-Pbca, a=5.436 Å, b=9.166 Å, c=5.135 Å [44])

Other structures exist as well, for example, cotunnite TiO_2 has been synthesized at high pressures and is one of the hardest polycrystalline materials known [45].

However, only rutile and anatase play any role in the applications of TiO_2 and are of any interest here as they have been studied with surface science techniques. Their unit cells are shown in Fig. 2. In both structures, the basic building block consists of a titanium atom surrounded by six oxygen atoms in a more or less distorted octahedral configuration. In each structure, the two bonds between the titanium and the oxygen atoms at the aspices of the octahedron are slightly longer. A sizable deviation from a 90° bond angle is observed in anatase. In rutile, neighboring octahedra share one corner along ⟨110⟩ – type directions, and are stacked with their long axis alternating by 90°. In anatase the corner-sharing octahedra form (0 0 1) planes. They are connected with their edges with the plane of octahedra below. In all three TiO_2 structures, the stacking of the octahedra results in threefold coordinated oxygen atoms [46].

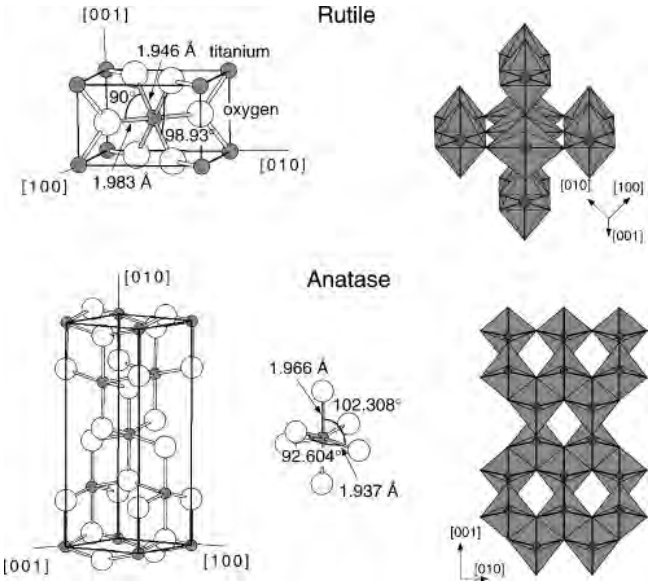

Figure 2: Unit cells of rutile and anatase [46]

.

TiO_2 is a n-type semiconductor [47]. The parameters of TiO_2 lattice at different temperatures are given in Table 1 [48]. Comparison of properties of anatase and rutile is given in Table 2 [49].

TiO_2 itself is not a magnetic material, but when it doped by a few percent of Co dioxide titanium becomes a ferromagnetic [60, 61].

Dark Processes in TiO_2

For semiconductor surface in contact with vacuum surface states are formed. These surfaces alter the electronic structure drastically [47]. As dioxide titanium is covalently bound semiconductor so it has covalent surface states (Shotkey states). Surface states on clean surfaces originate from dangling bonds [62]. These surface states introduce additional energy levels in the middle of the bandgap. To achieve electronic equilibrium between the surface and bulk, a positively charged space charged layer is formed just beneath the surface of an n-type semiconductor [21]. Also, usually, the defects on the TiO_2 surfaces exist in the form of O_vs (s – means surface) by removing surface lattice oxygen atoms in the preparation procedure, leaving behind unpaired electrons (in the Ti 3d orbitals) on the surfaces [63]. These two effects gives the band binding as illustrated on Fig. 3 [46].

Point defects, including O_vs, interstitial titanium ions (Ti^{3+}) and substituted ions, exist in all the crystalline materials of TiO_2. Vacancies and interstitial ions are intrinsic defects of crystalline materials, which may significantly affect the catalytic property, mass transport, and electrical conduction of the materials. The point defects introduce new electronic states in the bandgap of TiO_2, which are called as defect states. The positions of defect states in the bandgap are affected by the phases and surface structures of TiO_2. For example, the defect states of R-TiO_2(110) are located at $\approx 0.8 - 1.0\ eV$ below the CB edge [64]. However, the defect states of A-TiO_2(101) are located at $\approx 0.4 - 1.1\ eV$ below the CB edge [65–69]. Different types of deffects in TiO_2 are shown on Fig. 4 [70].

For realistic cases, when electron-rich TiO_2 surfaces adsorb different types of adsorbates, charge transfer between surfaces and adsorbates will occur, which may even revert the direction of band bending [69].

Table 1: The parameters of TiO_2 lattice at different temperatures

Lattice parameters		Temperature, °C
Dimensions	Lattice constant, Å	
a	3.7845	28
c	9.5143	
a	3.7855	84
c	9.5185	
a	3.7866	161
c	9.5248	
a	3.7875	210
c	9.5294	
a	3.7884	258
c	9.5342	
a	3.7894	306
c	9.5374	
a	3.7907	354
c	9.5432	
a	3.7923	449
c	9.5548	
a	3.7939	497
c	9.5595	
a	3.7948	534
c	9.5669	
a	3.7962	571
c	9.5754	
a	3.7970	608
c	9.5794	
a	3.7989	645
c	9.5872	
a	3.7998	679
c	9.5933	
a	3.8009	712
c	9.5975	

Table 2: Properties of anatase and rutile

Property	Anatase	Rutile	Reference
Crystal structure	Tetragonal	Tetragonal	[50]
Atoms per unit cell (Z)	4	2	[51]
Space group	$I\frac{4}{\alpha}md$	$P\frac{4_2}{m}nm$	[52]
Type of band gap	indirect	direct	[53]
Lattice parameters (nm)	a = 0.3785	a = 0.4594	
	c = 0.9514	c = 0.29589	[51]
Unit cell volume (nm^3)	0.1363	0.0624	[51]
Density (kg/m^3)	3894	4250	[51]
Calculated band gap			
(eV)	3.23–3.59	3.02–3.24	[54–57]
(nm)	345.4–383.9	382.7–410.1	
Experimental band gap			
(eV)	$\sim$ 3.2	$\sim$ 3.0	[56, 58]
(nm)	$\sim$ 387	$\sim$ 413	
Refractive index	2.54, 2.49	2.79, 2.903	[50]
Solubility in HF	Soluble	Insoluble	[59]
Solubility in H_2O	Insoluble	Insoluble	[50]
Hardness (Mohs)	5.5–6	6–6.5	[49]
Bulk modulus (GPa)	183	206	[57]

The accumulation of electrons at the surface determines the surface chemistry of TiO_2. All processes occurring at the surface of semiconductors are driven to achieve an equilibrium between the Fermi level potential and the chemical potential of the adsorbates, with the position of the Fermi level being equal to the work function of the semiconductor [21].

Deskins et al. [70] suggested that the relative electronegativity of TiO_2 surfaces and adsorbates may perhaps be the key parameter to understand the charge transfer between TiO_2 surfaces and adsorbates. Based on their theoretical works, electron transfer from the TiO_2 surface to adsorbates only occurs when the electronegativity of adsorbates ($\chi_{adsorbate}$) is larger than that of TiO_2 (χ_{TiO_2}) (Figure 5a). Otherwise, no charge transfer occurs (Figure 5b).

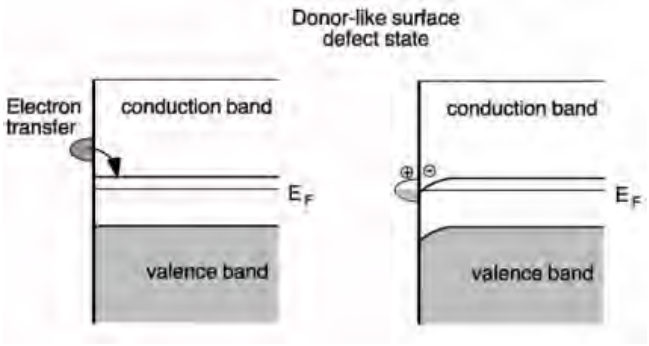

Figure 3: Schematic diagram of the band-bending effect due to donor-like surface defect states. Surface oxygen vacancies create a defect state and electrons are donated to the system. A charge accumulation layer is created in the near-surface region and the bands in the n-type semiconducting TiO_2 sample bend downwards.

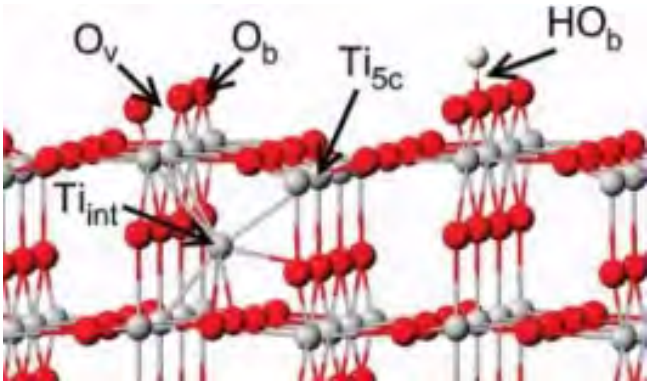

Figure 4: Structure of the rutile (110) surface. Red spheres represent O atoms, gray spheres represent Ti atoms, and white spheres represent H atoms. The notable surface sites are the bridging row O atoms (O_b) and the five-coordinated Ti sites (Ti_{5c}). Also shown are defects that lead to surface reduction: O vacancies (O_v), surface hydroxyls (HO_b), and interstitial Ti atoms (Ti_{int}).

Illumination of TiO_2

When exposed to light (sun- or ultraviolet- light), the semiconductor absorbs photons with sufficient energy (more or equal to band gap energy) to inject electrons from the valence band to its conduction band, creating electron/hole pairs [47] as shown on Fig. 6. As magnitude of the band gap for TiO_2 semiconductor is $\sim 3.2\ eV$ for anatase modification and $\sim 3.0\ eV$ for rutile modification, so there is wavelength threshold of $\lambda < 388\ nm$ for anatase and $\lambda < 414\ nm$ for rutile to become electronically conductive. It should be noted that in sunlight the percentage of ultraviolet is about 3 % [71].

Photocatalytic reactions can only occur at the TiO_2 surface. After migration to surface of TiO_2 electrons e^- and holes h^+ can oxidize and reduce absorbed molecules, respectively. Some of electrons and holes are recombined. In fact, time-resolved spectroscopy studies reveal that the most of photogenerated e^-/h^+ pairs (~ 90 %) recombine rapidly after excitation. This is assumed to be one reason for the relatively low values of photonic efficiency ζ (the rate of the formation of the reaction products divided by the incident flow) [21].

Schematically these steps are shown on Fig 7 [72] and in the following table [73]:

Table 3: Schematic model illustrating the main steps associated with TiO_2 photocatalysis

No of step	Reaction	Time
1	Charge carrier generation: $TiO_2 \xrightarrow{h\nu} TiO_2(e^-_{CB} + h^+_{VB})$ and thermalization: $e^{-*} \rightarrow e^- + heat(phonons)$ $h^{+*} \rightarrow h^+ + heat(phonons)$	<100 fs 10 fs
2	Trapping CB electrons (e^-_{cb}) at defect Ti^{4+} sites: $Ti^{4+}_{ds} + e^-_{cb} \rightarrow Ti^{3+}_{ds}$ [74]	200 fs
3	Trapping valence band holes (h^+_{vb}) at terminal Ti–OH or surface Ti–O–Ti sites: $Ti - O_sH\ or\ Ti - Os - Ti + h^+_{vb} \rightarrow Ti - O_sH^{\cdot +}\ or\ Ti - O^{\cdot +}_s - Ti$ [74]	200 fs
4	Reduction of adsorbed electron acceptor (A_{ad}) with e^-_{cb} at reduction sites: $e^-_{cb} + A_{ad} \rightarrow A^{\cdot -}_{ad}$	>10 ns
5	Reduction of A_{ad} with electrons trapped at defect sites (Ti^{3+}_{ds}): $Ti^{3+}_{ds} + A_{ad} \rightarrow Ti^{4+}_{ds} + A^{\cdot -}_{ad}$	slow process

6	Oxidation of adsorbed electron donor (D_{ad}) by trapped holes at oxidation sites: $Ti-O_sH^{\cdot+}$ *or* $Ti-O_s^{\cdot+}-Ti+D_{ad}\rightarrow Ti-O_sH$ *or* $Ti-O_s-Ti+D_{ad}^{\cdot+}$		100 ps-10 ns
7	Recombination of e_{cb}^- with trapped holes [75]:		
	$e_{cb}^-+Ti-O_sH^{\cdot+}$ *or* $Ti-O_s^{\cdot+}-Ti\rightarrow Ti-O_sH$ *or* $Ti-O_s-Ti$	*rutile* *anatase*	24 *ns* $\sim$ *few ms*
8	Recombination of Ti_{ds}^{3+} with trapped holes [75]:		
	$Ti_{ds}^{3+}+Ti-O_sH^{\cdot+}$ *or* $Ti-O_s^{\cdot+}-Ti\rightarrow Ti_{ds}^{4+}+Ti-O_sH$ *or* $Ti-O_s-Ti$	*rutile* *anatase*	[48 *ns*] [$\sim$ *few ns*]

Charge carrier generation and thermalization

Charge carrier generation in anatase and rutile is running in different ways because anatase belongs to indirect band gap semiconductor, rutile - to direct one [76]. The schemes of direct and indirect band gaps are shown on Fig. 8a. Indirect transitions involve either the absorption of both a photon and a phonon or the absorption of a photon and the emission of a phonon. The conditions for indirect transitions, as shown in Fig. 8a, can be summarized in the following way [76]. For the conservation of momentum,

$$k_{ph}=k_f-k_i$$

where k_{ph} is the wave vector for the phonon, and k_f and k_i are the wave vectors for the final and initial states of the transition, respectively.

For direct transitions $k_{ph}=0$ and for indirect transitions $k_{ph}\neq 0$.

After illumination of TiO_2 by UV photons with energy more or equal to band gap width free electrons and holes are generated (fig. 6). It should be noted that the penetration depth δ_p of ultraviolet light in TiO_2 is approximately equal to 160 nm [77]. Therefore electron-hole pairs are generated in the outer surface region of the TiO_2. Due to the near surface electric field the recombination of e^-/h^+ is retarded [21].

Continuous illumination will result in the annihilation of this electric field, that is, a band flattening [78]. Yates et al. [21, 79] explained the appearance of this band flattening by a band shifting at the surface, because the free electrons move to the bulk, while free holes accumulate at the surface where the negative charge is neutralized. However, band flattening can also be explained by a band shifting in the bulk region, as the number of electrons increases in the bulk upon illumination.

According to electron paramagnetic resonance (EPR) spectroscopy process of pair generation occurs in femtoseconds [80] (1 fs = $10^{-15}s$) up to 100 fs. But it is obviously that e^-/h^+ pair generation time for indirect and direct TiO_2 modifications(anatase and rutile, respectively) is differ. There is no data in literature concerning this difference in time of the charge carrier generation.

In an ideal photocatalyst, all photon energy invested in charge carrier generation would be available for redox reactions, namely, hot electrons (or deep holes) produced by shorter wavelength light have more reductive (or oxidative) capacity than those at the band edges of a photocatalyst [69]. However, charge carrier thermalization occurs rapidly.

After e^-/h^+ generation the energetic electrons continue to travel in the solid, losing its energy and producing shallower core holes. This cascade process, often called "thermalization", is repeated until the hole is created at the top of valence band and fully thermalized electrons settling in the bottom of the conduction band [81].

In [82] authors found that time of thermalization in TiO_2 (110) is equal to 10 fs.

These studies clearly demonstrate that charge carrier thermalization occurs prior to recombination or transfer.

Electron and hole trapping

Once produced, the charge carriers become trapped, either in shallow traps (ST) or in deep traps (DT) [80]. The photogenerated charge carriers can be trapped in either in bulk or on the surface. In generally, surface trapping at either the subsurface or the surface region is preferred in semiconductor nanoparticles [83, 84].

Because of the upward band bending in n-type TiO_2, the photogenerated electrons are forced to move from its surface into the bulk, where they can be delocalized over different Ti sites. Both theoretical and experimental studies are predicting bulk (subsurface) trapping rather than surface trapping of these electrons [85–87]. However, alternative studies also exist demonstrating that $Ti^{4+}OH$ groups located at the TiO_2 surface can act as trapping centers for the electrons, resulting in the formation of $Ti^{3+}OH$ species. Such species can attract holes, thus behaving as recombination centers [88–90].

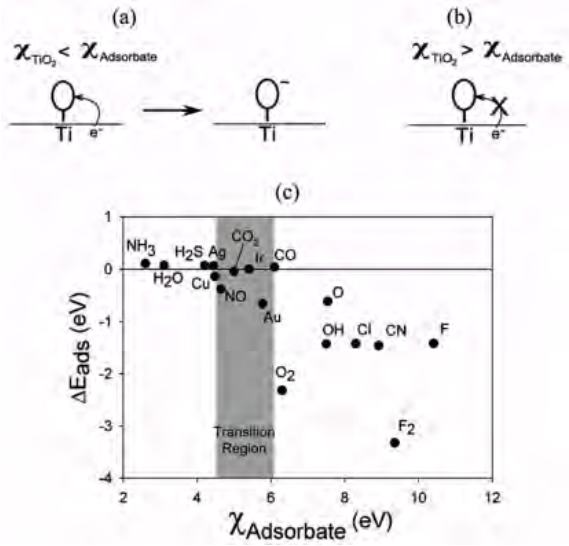

Figure 5: The effect of electronegativity on the adsorption energy of adsorbates on TiO_2.

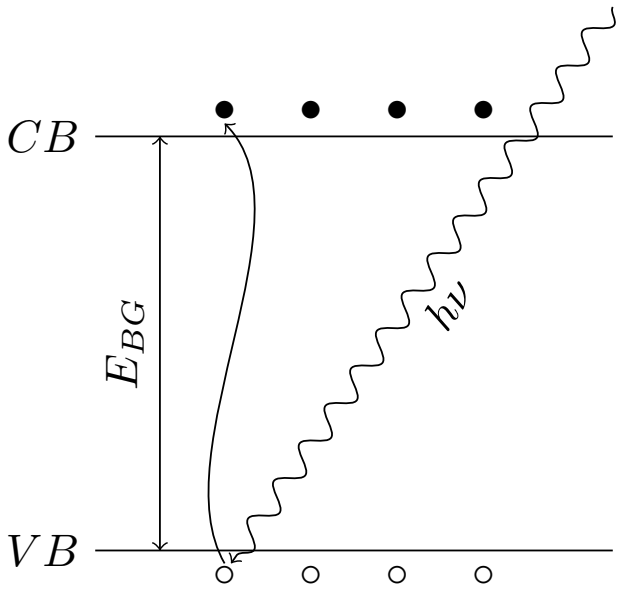

Figure 6: Scheme of electron/hole formation in the semiconductors. CB - conduction band, VB – valence band, E_{BG} – energy band gap, ○ - holes, ● - electrons, $h\nu$ - photon.

Upon 355 nm excitation, photogenerated electrons and holes are trapped very rapidly within 100 fs. However, the excess energy of free electrons in the TiO_2 CB slows the trapping time to ≈200 fs upon 266 nm irradiation [91].

Reduction of electron acceptors A_{ad} with electrons and oxidation of adsorbed electron donor D_{ad} by holes

Following their formation by light excitation, electrons and holes can easily be transferred to electron and hole acceptors, respectively. The quantum efficiency of these reactions depends on the charge-transfer rate at the interface, on the recombination rate within the particle, and on the transit time of the photogenerated charge carriers to the surface [21].

Photocatalytic reactions occur on the surface of semiconductor. Photocatalytic reactions can be reduction and oxidation ones. These reactions are form reactive oxygen species (ROS), such as superoxide anion radicals ($O_2^{\cdot -}$), hydroperoxy radicals ($\cdot OOH$), hydrogen peroxide (H_2O_2), and hydroxyl radicals ($\cdot OH$), under both aqueous and aerated conditions [21, 92]. These ROS play a crucial role in the photocatalysis on TiO_2 for water purification, air cleaning, self-cleaning, self-sterilization, etc. The reduction reactions on photo-irradiated TiO_2 under acidic conditions can be depicted as follows [21, 73, 92, 93]:

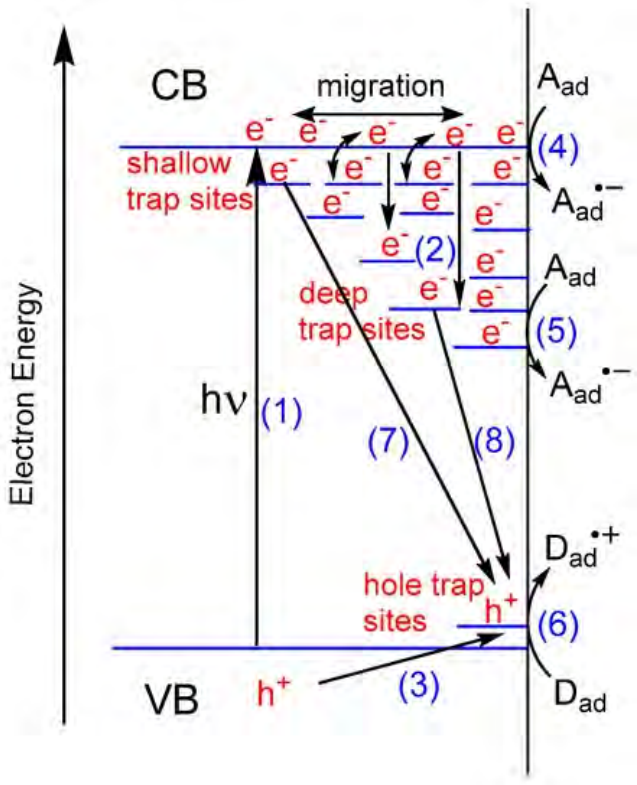

Figure 7: Schematic model illustrating the main steps associated with TiO_2 photocatalysis

Photoreduction: $O_2 + (Ti^{3+}_{ds} \ and \ e^-_{cb}) \rightarrow O_2^{\cdot -}$

Protonation: $O_2^{\cdot -} + H^+ \rightarrow \cdot OOH$

Disproportionation: $2 \cdot OOH \rightarrow H_2O_2 + O_2$

Photoreduction: $H_2O_2 + (Ti^{3+}_{ds} \ and \ e^-_{cb}) \rightarrow \cdot OH + OH^-$

In oxidation reactions hydroxyl radicals OH are formed via direct hole oxidation of adsorbed H_2O [94]:

$$h^+ + H_2O \rightarrow \cdot OH$$

There are two types of $\cdot OH$ radicals: free mobile (OH_f) and surface bound (OH_s) hydroxyl radicals, which exhibit different reactivities depending on the properties of target pollutants. The OH_f generation and the subsequent diffusion from the surface are critical in achieving the mineralization of non-adsorbing substrates by extending the reaction zone from the surface to the solution bulk [95].

For environmental application main role plays free hydroxyl radical OH_f. As mentioned in [95] these radicals are producing mainly by anatase modification of titanium dioxide.

The electron-hole recombination

The electron-hole recombination process is undesirable one because it reduce efficiency of photochemical reactions occurring on the surface of TiO_2. As it was above mentioned about 90 % of charge carriers recombine decreasing efficiency of the photocatalytic reactions.

The electron-hole recombination is found to be quite rapid cases, with a majority of recombination complete within 50 ps[96]. In [97] revealed significantly higher yields and longer lifetimes of charge carriers in the anatase powder. Yamada et al [75] stated that electrons lifetime in rutile is equal to 24 ns, in anatase - microseconds; lifetime of holes in rutile is equal to 48 ns, in anatase - nanoseconds. The longer charge carriers lifetime in anatase is one of the main reason why anatase has more photoactivity property.

There are three basic recombination mechanisms that are responsible for carrier annihilation in a semiconductor [98]:

1. band-to-band recombination, which occurs when an electron moves from the conduction band (CB) to the empty valence band (VB) containing a hole (the rate of band-to-band recombination depends on

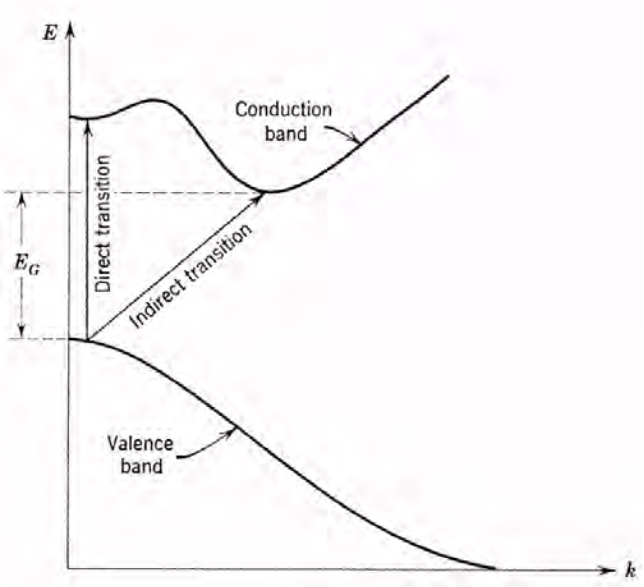

(a) Direct and indirect transitions between valence and conduction bands with extrema at different values of k.

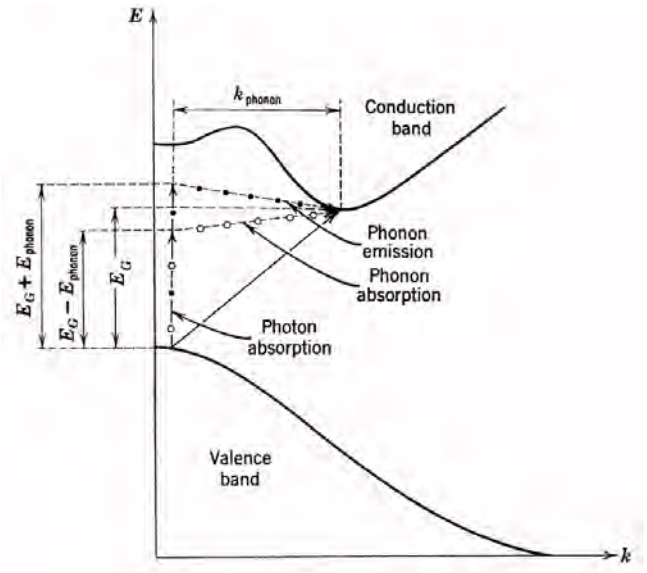

(b) Indirect transitions between conduction and valence bands with extrema at different values of k. Two processes are possible, one involving the absorption of a photon and a phonon, and the other involving the absorption of a photon and the emission of a phonon.

Figure 8: Direct and indirect transitions between valence and conduction bands [76].

the product of the concentrations of available electrons and holes and is second order in charge carrier concentration];

2. trap-assisted recombination (Shockley-Read-Hall Model, SRH model),which occurs when an electron in the CB recombines indirectly with a hole in the VB at a "trap" state;
3. Auger recombination, which occurs when an electron-hole pair recombine in a band-to-band transition giving off the generated energy to another electron or hole.

The electron-hole recombination process reaction successfully compete with the hole-transfer [99].

As it was mentioned earlier time of electron-pair recombination in rutile shorter than in anatase. This is one of the main reason why anatase is more photoactive. Thi is because of that anatase has indirect band gap and to recombine the

OH generation

CONCLUSION

In the article the difference between anatase and rutile was considered as from photocatalytic point of view as well as from structure point of view. The main differences are

- Cell volume of rutile smaller then anatase one by factor ≈ 2.
- Rutile is more stable modification of dioxide titanium in comparison with anatase.
- Width of band gap in anatase is equal to 3.2 eV (388 nm - ultraviolet light), meanwhile, rutile has width of band gap equal to 3.0 eV that corresponds to 414 nm that is in visible diapason of light.
- Anatase has indirect transitions between conduction and valence bands, rutile - direct.
- Recombination of electron/hole pairs is quicker in rutile then in anatase because recombination in anatase slower because it has indirect transition in band gap.
- Free radical OH_f can be generated by anatase only.

Thus, anatase has more photocatalytic activity in comparison with rutile because of more longer lifetime of charge carriers. But the width of rutile band gap is narrower so rutile has photocatalytic properties in visible diapason of light - the aim of last decade of investigations. It is desire to increase time life of electrons and holes in rutile. It can be done by external forces, for example electric or magnetic fields.

ORCID IDs

Volodymyr Morgunov, https://orcid.org/0000-0002-8681-1941,
Serhii Lytovchenko, https://orcid.org/0000-0002-3292-5468,
Volodymyr Chyshkala, https://orcid.org/0000-0002-8634-4212,
Dmytro Riabchykov, https://orcid.org/0000-0002-9529-0412,
Dementii Matviienko, https://orcid.org/0000-0001-9862-5815.

REFERENCES

[1] A. Fujishima and K. Honda, Nature **238**, 37–38 (1972), https://doi.org/10.1038/238037a0.

[2] T. Ochiai and A. Fujishima, Journal of Photochemistry and photobiology C: Photochemistry reviews **13**, 247–262 (2012), https://doi.org/10.1016/j.jphotochemrev.2012.07.001.

[3] F. He, W. Jeon, and W. Choi, Nature Communications **12**, 1–4 (2021), https://doi.org/10.1038/s41467-021-22839-0.

[4] A Fernandez, G Lassaletta, V. Jimenez, A Justo, A. Gonzalez-Elipe, J.-M. Herrmann, H Tahiri, and Y Ait-Ichou, Applied Catalysis B: Environmental **7**, 49–63 (1995), https://doi.org/10.1016/0926-3373(95)00026-7.

[5] K. Nakata, T. Ochiai, T. Murakami, and A. Fujishima, Electrochimica Acta **84**, ELECTROCHEMICAL SCIENCE AND TECHNOLOGYState of the Art and Future PerspectivesOn the occasion of the International Year of Chemistry (2011), 103–111 (2012), https://doi.org/10.1016/j.electacta.2012.03.035.

[6] J. Ângelo, L. Andrade, L. M. Madeira, and A. Mendes, en, Journal of Environmental Management **129**, 522–539 (2013), https://doi.org/10.1016/j.jenvman.2013.08.006.

[7] O. Ola and M. M. Maroto-Valer, en, Journal of Photochemistry and Photobiology C: Photochemistry Reviews **24**, 16–42 (2015), https://doi.org/10.1016/j.jphotochemrev.2015.06.001.

[8] G. Fu, P. S. Vary, and C.-T. Lin, The Journal of Physical Chemistry B **109**, 8889–8898 (2005), https://doi.org/10.1021/jp0502196.

[9] Y. Liu, X. Wang, F. Yang, and X. Yang, en, Microporous and Mesoporous Materials **114**, 431–439 (2008), https://doi.org/10.1016/j.micromeso.2008.01.032.

[10] U. Joost, K. Juganson, M. Visnapuu, M. Mortimer, A. Kahru, E. Nõmmiste, U. Joost, V. Kisand, and A. Ivask, en, Journal of Photochemistry and Photobiology B: Biology **142**, 178–185 (2015), https://doi.org/10.1016/j.jphotobiol.2014.12.010.

[11] A. Kubacka, M. Ferrer, M. L. Cerrada, C. Serrano, M. Sánchez-Chaves, M. Fernández-García, A. de Andrés, R. J. J. Riobóo, F. Fernández-Martín, and M. Fernández-García, en, Applied Catalysis B: Environmental **89**, 441–447 (2009), https://doi.org/10.1016/j.apcatb.2009.01.002.

[12] S. Sfaelou and P. Lianos, AIMS Mater. Sci. **3**, 270–288 (2016).

[13] M. Kaneko, N. Gokan, N. Katakura, Y. Takei, and M. Hoshino, Chem. Commun., 1625–1627 (2005), https://doi.org/10.1039/B418580C.

[14] K. Iyatani, Y. Horiuchi, M. Moriyasu, S. Fukumoto, S.-H. Cho, M. Takeuchi, M. Matsuoka, and M. Anpo, J. Mater. Chem. **22**, 10460–10463 (2012), https://doi.org/10.1039/C2JM32064A.

[15] M. Ni, M. K. Leung, D. Y. Leung, and K. Sumathy, Renewable Sustainable Energy Rev. **11**, 401–425 (2007), https://doi.org/10.1016/j.rser.2005.01.009.

[16] V. Kumaravel, S. Mathew, J. Bartlett, and S. C. Pillai, Applied Catalysis B: Environmental **244**, 1021–1064 (2019), https://doi.org/10.1016/j.apcatb.2018.11.080.

[17] S. Banerjee, D. D. Dionysiou, and S. C. Pillai, Applied Catalysis B: Environmental **176-177**, 396–428 (2015), https://doi.org/10.1016/j.apcatb.2015.03.058.

[18] C. Euvananont, C. Junin, K. Inpor, P. Limthongkul, and C. Thanachayanont, Ceramics International **34**, The Fifth Asian Meeting on Electroceramics (AMEC-5), 1067–1071 (2008), https://doi.org/10.1016/j.ceramint.2007.09.043.

[19] A. Folli, C. Pade, T. B. Hansen, T. De Marco, and D. E. Macphee, Cement and Concrete Research **42**, 539–548 (2012), https://doi.org/10.1016/j.cemconres.2011.12.001.

[20] C. Garlisi and G. Palmisano, en, Applied Surface Science **420**, 83–93 (2017), https://doi.org/10.1016/j.apsusc.2017.05.077.

[21] J. Schneider, M. Matsuoka, M. Takeuchi, J. Zhang, Y. Horiuchi, M. Anpo, and D. W. Bahnemann, Chemical reviews **114**, 9919–9986 (2014), https://doi.org/10.1021/cr5001892.

[22] O. Carp, C. L. Huisman, and A. Reller, en, Progress in Solid State Chemistry **32**, 33–177 (2004), https://doi.org/10.1016/j.progsolidstchem.2004.08.001.

[23] M. Yadav, A. Yadav, R. Fernandes, Y. Popat, M. Orlandi, A. Dashora, D. C. Kothari, A. Miotello, B. L. Ahuja, and N. Patel, en, Journal of Environmental Management **203**, 364–374 (2017), https://doi.org/10.1016/j.jenvman.2017.08.010.

[24] K. Subalakshmi and J. Senthilselvan, en, Solar Energy **171**, 914–928 (2018), 10.1016/j.solener.2018.06.077.

[25] M. Diak, E. Grabowska, and A. Zaleska, en, Applied Surface Science **347**, 275–285 (2015), https://10.1016/j.apsusc.2015.04.103.

[26] X. Pan and Y.-J. Xu, The Journal of Physical Chemistry C **117**, 17996–18005 (2013), 10.1021/jp4064802.

[27] Z. Jiang, H. Wang, H. Huang, and C. Cao, en, Chemosphere **56**, 503–508 (2004), https://doi.org/10.1016/j.chemosphere.2004.02.006.

[28] V. Morgunov and D. Rudenko, *Method of photocatalytic disinfection and purification of air from harmful gas compounds, dust*, UA Patent 108560, Jul. 2016.

[29] K.-H. Chung, S. Jeong, B.-J. Kim, K.-H. An, Y.-K. Park, and S.-C. Jung, en, International Journal of Hydrogen Energy **43**, 11422–11429 (2018), https://doi.org/10.1016/j.ijhydene.2018.03.190.

[30] J. F. Gomes, A. Lopes, K. Bednarczyk, M. Gmurek, M. Stelmachowski, A. Zaleska-Medynska, M. E. Quinta-Ferreira, R. Costa, R. M. Quinta-Ferreira, and R. C. Martins, en, ChemEngineering **2**, 4 (2018), https://doi.org/10.3390/chemengineering2010004.

[31] N. Singhal and U. Kumar, en, Molecular Catalysis **439**, 91–99 (2017), https://doi.org/10.1016/j.mcat.2017.06.031.

[32] J. Choi, H. Park, and M. R. Hoffmann, The Journal of Physical Chemistry C **114**, 783–792 (2010), https://doi.org/10.1021/jp908088x.

[33] J. M. Macák, H. Tsuchiya, A. Ghicov, and P. Schmuki, en, Electrochemistry Communications **7**, 1133–1137 (2005), https://doi.org/10.1016/j.elecom.2005.08.013.

[34] G. Yang, Z. Yan, and T. Xiao, en, Applied Surface Science **258**, 8704–8712 (2012), https://doi.org/10.1016/j.apsusc.2012.05.078.

[35] A. Zaleska, Recent Patents on Engineering **2**, 157–164 (2008), https://doi.org/10.2174/187221208786306289.

[36] S. G. Kumar and K. S. R. K. Rao, en, Applied Surface Science, 2nd International Symposium on Energy and Environmental Photocatalytic Materials **391**, 124–148 (2017), https://doi.org/10.1016/j.apsusc.2016.07.081.

[37] N. Serpone and A. V. Emeline, en, International Journal of Photoenergy **4**, 91–131 (2002), https://dpoi.org/10.1155/S1110662X02000144.

[38] S. E. Braslavsky and K. N. Houk, de, Pure and Applied Chemistry **60**, 1055–1106 (1988), https://doi.org/10.1351/pac198860071055.

[39] J. W. Verhoeven, de, Pure and Applied Chemistry **68**, 2223–2286 (1996), https://doi.org/10.1351/pac199668122223.

[40] S. E. Braslavsky, A. M. Braun, A. E. Cassano, A. V. Emeline, M. I. Litter, L. Palmisano, V. N. Parmon, and N. Serpone, de, Pure and Applied Chemistry **83**, 931–1014 (2011), https://doi.org/10.1351/PAC-REC-09-09-36.

[41] R. M. Wood, Proceedings of the Physical Society (1958-1967) **80**, 783 (1962), https://doi.org/10.1088/0370-1328/80/3/323.

[42] C. A. Hampel, *The encyclopedia of the chemical elements,* English, OCLC: 449569 (Reinhold Book Corp., New York, 1968).

[43] F. Grant, Reviews of Modern Physics **31**, 646–674 (1959), https://doi.org/10.1103/RevModPhys.31.646.

[44] G. V. Samsonov, *The Oxide Handbook*, en, IFI Data Base Library (Springer US, 1973),https://doi.org/10.1007/978-1-4615-9597-7.

[45] L. Dubrovinsky, N. Dubrovinskaia, V. Swamy, J. Muscat, N. Harrison, R. Ahuja, B. Holm, and B. Johansson, Nature **410**, 653–654 (2001), https://doi.org/10.1038/35070650.

[46] U. Diebold, en, Surface Science Reports **48**, 53–229 (2003), https://doi.org/10.1016/S0167-5729(02)00100-0.

[47] S. M. Bard A J and S Licht, *Encyclopedia of electrochemistry. Vol. 6. Semiconductor electrodes and photoelectrochemistry*, 2002.

[48] K. V. K. Rao, S. V. N. Naidu, and L. Iyengar, en, Journal of the American Ceramic Society **53**, 124–126 (1970), https://doi.org/10.1111/j.1151-2916.1970.tb12051.x.

[49] D. A. H. Hanaor and C. C. Sorrell, en, Journal of Materials Science **46**, 855–874 (2011), https://doi.org/10.1007/s10853-010-5113-0.

[50] T. Jones, J. Edwards, and J. Kallioinen, en, in *Kirk-Othmer Encyclopedia of Chemical Technology* (American Cancer Society, 2019), pp. 1–76,https://doi.org/10.1002/0471238961.0914151805070518.a01.pub4.

[51] J. K. Burdett, T. Hughbanks, G. J. Miller, J. W. Richardson, and J. V. Smith, Journal of the American Chemical Society **109**, 3639–3646 (1987), https://doi.org/10.1021/ja00246a021.

[52] T. Hahn and P. Paufler, en, Crystal Research and Technology **19**, 1306–1306 (1984), https://doi.org/10.1002/crat.2170191008.

[53] J. Zhang, P. Zhou, J. Liu, and J. Yu, en, Physical Chemistry Chemical Physics **16**, 20382–20386 (2014), https://doi.org/10.1039/C4CP02201G.

[54] K Madhusudan Reddy, S. V. Manorama, and A Ramachandra Reddy, en, Materials Chemistry and Physics **78**, 239–245 (2003), https://doi.org/10.1016/S0254-0584(02)00343-7.

[55] N. Serpone, The Journal of Physical Chemistry B **110**, 24287–24293 (2006), https://doi.org/10.1021/jp065659r.

[56] N. Daude, C. Gout, and C. Jouanin, Physical Review B **15**, 3229–3235 (1977), https://doi.org/10.1103/PhysRevB.15.3229.

[57] H. Wang and J. P. Lewis, en, Journal of Physics: Condensed Matter **18**, 421–434 (2005), https://doi.org/10.1088/0953-8984/18/2/006.

[58] D. Mardare, M. Tasca, M. Delibas, and G. I. Rusu, en, Applied Surface Science **156**, 200–206 (2000), https://doi.org/10.1016/S0169-4332(99)00508-5.

[59] T. Ohno, K. Sarukawa, and M. Matsumura, The Journal of Physical Chemistry B **105**, 2417–2420 (2001), https://doi.org/10.1021/jp003211z.

[60] S. Chambers, S. Thevuthasan, R. Farrow, R. Marks, J. Thiele, L. Folks, M. Samant, A. Kellock, N. Ruzycki, D. Ederer, and U. Diebold, Applied Physics Letters **79**, 3467–3469 (2001), https://doi.org/10.1063/1.1420434.

[61] Y. Matsumoto, M. Murakami, T. Shono, T. Hasegawa, T. Fukumura, M. Kawasaki, P. Ahmet, T. Chikyow, S.-Y. Koshihara, and H. Koinuma, Science **291**, 854–856 (2001), https://doi.org/10.1126/science.1056186.

[62] W. Mönch, *Semiconductor Surfaces and Interfaces*, en, 3rd ed., Springer Series in Surface Sciences (Springer-Verlag, Berlin Heidelberg, 2001),https://doi.org/10.1007/978-3-662-04459-9.

[63] P. J. D. Lindan, N. M. Harrison, M. J. Gillan, and J. A. White, Physical Review B **55**, 15919–15927 (1997), https://doi.org/10.1103/PhysRevB.55.15919.

[64] Z. Wang, B. Wen, Q. Hao, L.-M. Liu, C. Zhou, X. Mao, X. Lang, W.-J. Yin, D. Dai, A. Selloni, and X. Yang, Journal of the American Chemical Society **137**, 9146–9152 (2015), https://doi.org/10.1021/jacs.5b04483.

[65] B. Wen, Q. Hao, W.-J. Yin, L. Zhang, Z. Wang, T. Wang, C. Zhou, A. Selloni, X. Yang, and L.-M. Liu, en, Physical Chemistry Chemical Physics **20**, 17658–17665 (2018), https://doi.org/10.1039/C8CP02648C.

[66] W.-J. Yin, B. Wen, C. Zhou, A. Selloni, and L.-M. Liu, en, Surface Science Reports **73**, 58–82 (2018), https://doi.org/10.1016/j.surfrep.2018.02.003.

[67] A. G. Thomas, W. R. Flavell, A. K. Mallick, A. R. Kumarasinghe, D. Tsoutsou, N. Khan, C. Chatwin, S. Rayner, G. C. Smith, R. L. Stockbauer, S. Warren, T. K. Johal, S. Patel, D. Holland, A. Taleb, and F. Wiame, Physical Review B **75**, 035105 (2007), https://doi.org/10.1103/PhysRevB.75.035105.

[68] M. Setvin, C. Franchini, X. Hao, M. Schmid, A. Janotti, M. Kaltak, C. G. Van de Walle, G. Kresse, and U. Diebold, Physical Review Letters **113**, 086402 (2014), https://doi.org/10.1103/PhysRevLett.113.086402.

[69] Q. Guo, C. Zhou, Z. Ma, and X. Yang, en, Advanced Materials **31**, 1901997 (2019), https://doi.org/10.1002/adma.201901997.

[70] N. A. Deskins, R. Rousseau, and M. Dupuis, The Journal of Physical Chemistry C **114**, 5891–5897 (2010), https://doi.org/10.1021/jp101155t.

[71] R. R. D. Center, ASTM G173-03 Tables (2012).

[72] M. A. Henderson, en, Surface Science Reports **66**, 185–297 (2011), 10.1016/j.surfrep.2011.01.001.

[73] S. Kohtani, A. Kawashima, and H. Miyabe, en, Catalysts **7**, 303 (2017), https://doi.org/10.3390/catal7100303.

[74] Y. Tamaki, A. Furube, M. Murai, K. Hara, R. Katoh, and M. Tachiya, en, Physical Chemistry Chemical Physics **9**, 1453–1460 (2007), https://doi.org/10.1039/B617552J.

[75] Y. Yamada and Y. Kanemitsu, Applied Physics Letters **101**, 133907 (2012), https://doi.org/10.1063/1.4754831.

[76] R. H. Bube, *Photoconductivity of solids* (Wiley, New York, 1978).

[77] D. M. Eagles, Journal of Physics and Chemistry of Solids **25**, 1243–1251 (1964), https://doi.org/10.1016/0022-3697(64)90022-8.

[78] J. M. Lantz and R. M. Corn, The Journal of Physical Chemistry **98**, 9387–9390 (1994), https://doi.org/10.1021/j100069a022.

[79] A. Stevanovic and J. T. Yates, The Journal of Physical Chemistry C **117**, 24189–24195 (2013), https://doi.org/10.1021/jp407765r.

[80] T. Berger, M. Sterrer, O. Diwald, E. Knözinger, D. Panayotov, T. L. Thompson, and J. T. Yates, The Journal of Physical Chemistry B **109**, 6061–6068 (2005), https://doi.org/10.1021/jp0404293.

[81] L. Liu and T.-K. Sham, en, in *Titanium dioxide - material for a sustainable environment*, edited by D. Yang (InTech, June 2018),https://doi.org/10.5772/intechopen.72856.

[82] L. Gundlach, R. Ernstorfer, and F. Willig, Physical Review B **74**, 035324 (2006), 10.1103/PhysRevB.74.035324.

[83] R. Qian, H. Zong, J. Schneider, G. Zhou, T. Zhao, Y. Li, J. Yang, D. W. Bahnemann, and J. H. Pan, en, Catalysis Today, Advances in photo(electro)catalysis for environmental applications and chemical synthesis **335**, 78–90 (2019), https://doi.org/10.1016/j.cattod.2018.10.053.

[84] A. Stevanovic and J. T. Yates, Langmuir **28**, 5652–5659 (2012), 10.1021/la205032j.

[85] T. Bredow and K. Jug, The Journal of Physical Chemistry **99**, 285–291 (1995), https://doi.org/10.1021/j100001a044.

[86] V. Shapovalov, E. V. Stefanovich, and T. N. Truong, en, Surface Science **498**, L103–L108 (2002), https://doi.org/10.1016/S0039-6028(01)01595-3.

[87] Y. Ji, B. Wang, and Y. Luo, The Journal of Physical Chemistry C **116**, 7863–7866 (2012), https://doi.org/10.1021/jp300753f.

[88] M. Anpo, T. Shima, and Y. Kubokawa, Chemistry Letters **14**, 1799–1802 (1985), https://doi.org/10.1246/cl.1985.1799.

[89] O. I. Micic, Y. Zhang, K. R. Cromack, A. D. Trifunac, and M. C. Thurnauer, The Journal of Physical Chemistry **97**, 7277–7283 (1993), https://doi.org/10.1021/j100130a026.

[90] C. Di Valentin, G. Pacchioni, and A. Selloni, Physical Review Letters **97**, 166803 (2006), https://doi.org/10.1103/PhysRevLett.97.166803.

[91] Y. Tamaki, K. Hara, R. Katoh, M. Tachiya, and A. Furube, The Journal of Physical Chemistry C **113**, 11741–11746 (2009), 10.1021/jp901833j.

[92] M. R. Hoffmann, S. T. Martin, W. Choi, and D. W. Bahnemann, Chemical Reviews **95**, 69–96 (1995), https://doi.org/10.1021/cr00033a004.

[93] H. H. Mohamed, R. Dillert, and D. W. Bahnemann, en, Journal of Photochemistry and Photobiology A: Chemistry **217**, 271–274 (2011), https://doi.org/10.1016/j.jphotochem.2010.09.024.

[94] P. F. Schwarz, N. J. Turro, S. H. Bossmann, A. M. Braun, A.-M. A. A. Wahab, and H. Duerr, The Journal of Physical Chemistry B **101**, 7127–7134 (1997), https://doi.org/10.1021/jp971315c.

[95] S. Kim and W. Choi, Environmental Science & Technology **36**, 2019–2025 (2002), https://doi.org/10.1021/es015560s.

[96] D. P. Colombo Jr and R. M. Bowman, The Journal of Physical Chemistry **99**, 11752–11756 (1995), https://doi.org/10.1021/j100030a020.

[97] K. M. Schindler and M. Kunst, Journal of Physical Chemistry **94**, 8222–8226 (1990), https://doi.org/10.1021/j100384a045.

[98] Z. Zhang and J. T. Yates, The Journal of Physical Chemistry C **114**, 3098–3101 (2010), 10.1021/jp910404e.

[99] D. P. Colombo and R. M. Bowman, The Journal of Physical Chemistry **100**, 18445–18449 (1996), https://doi.org/10.1021/jp9610628.

ПОРІВНЯННЯ ВЛАСТИВОСТЕЙ АНАТАЗА І РУТИЛА ДЛЯ ФОТОКАТАЛІТИЧНОГО ВИКОРИСТАННЯ: КОРОТКИЙ ОГЛЯД

В. В. Моргунов[a,b], **С. В. Літовченко**[a], **В. О. Чішкала**[a], **Д. Л. Рябчиков**[a], **Д. С. Матвієнко**[a]
[a] *Харківський національний університет імені В. Н. Каразіна, Пл. Свободи, 4, Харків, 61022, Україна;*
[b] *Українська інженерно-педагогічна академія, вул. Університетська, 16, Харків, 61003, Україна*

Діоксид титану (TiO_2) привертає велику увагу як напівпровідниковий фотокаталізатор через свою високу фотореактивність, нетоксичність, корозійну стійкість, фотостійкість, дешевизну. Він може бути використаний у широкому спектрі застосувань: очищення повітря та води, генерування водню (H_2), зменшення вмісту CO_2, у фотоелектричних пристроях тощо. Зусилля вчених були направлені на пошук способів, що використовують сонячне світло для фотокаталізу за допомогою діоксиду титану та підвищення фотокаталітичної ефективності. У цій статті ми розглядаємо різницю властивостей модифікацій анатазу та рутилу TiO_2. Анатаз має більш високу фотоефективність. Більш висока фотоефективність анатазу обумовлена більш тривалим терміном життя носіїв заряду (час життя e^-/h^+ в анатазі на 3 порядки вище, ніж у рутилу). Але анатаз має більшу ширину забороненої зони (3,2 еВ або 388 нм) у порівнянні з рутилом (3,0 еВ або 414 нм). Таким чином, анатаз стає світлочутливим в ультрафіолетовому (УФ) діапазоні світла, тим часом рутил - у фіолетовому спектрі видимого світла. Бажано отримати напівпровідник TiO_2 з властивостями, що поєднують найкращі як для анатазу так і для рутилу: більша фотореактивність та менша забороненої зони. Це можна зробити за допомогою зовнішніх факторів, таких як електричне або магнітне поле, легування тощо.

Ключові слова: фотокаталіз, діоксид титану, анатаз, рутил, ширина забороненої зони, фотоефективність, генерація електронних дірок.